Joint Workshop of the OS-Eval TT and CP-TT and SynObs Kick-Off
Tsukuba Center for Institutes
Nov 15-18, 2022

Coastal Ocean Data Assimilation with Fishing Vessels

Naoki HIROSE
RIAM, Kyushu University

Current ocean observation system

- Remote-sensing satellites
  - ✓ Basically measures ocean surface; inverse problem of subsurface and deep conditions
  - ✓ Accuracy near the coastline?
- Argo floats
  - ✓ Vertical profiles for deep ocean (~1000m)
  - ✓ Hardly measures shallow/coastal waters
- Limited measurement at subsurface levels near the coast

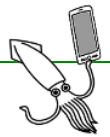

スマートCTD

スマートCTD　smart-ACT

“TEGARU” CTD sensor for international sale

今まで培ってきたCTD技術により汎用精度の安価型CTDを開発しました。
500mℓペットボトルサイズまで小型化し、煩わしい観測設定は不要としました。
観測データはBluetooth®無線技術でペアリングされたスマートフォンやタブレットにワンタッチで転送され、鉛直グラフや時系列グラフをその場で見ることができます。

特長：
①マグネットで簡単に電源ON-OFF操作が可能
②Bluetooth®無線技術で観測データをスマートフォンやタブレットに転送※1
③非接触充電採用
④独自のセンサーヘッド形状により、降下方向に制約なし
⑤漁業の合間でも観測できる簡単操作
⑥漁具に取付可能な堅固な構造
※1 OSはAndroid™6.0以上が必要です。

海洋・河川事業部

- お問い合わせフォーム
- 事業部ニュース
- スマートCTD
- 10筒採水器／4筒採水器
- 水中カメラ
- DEFIシリーズ
- RINKOシリーズ
- INFINITYシリーズ
- 多波長励起蛍光光度計

In-situ measurement with FV

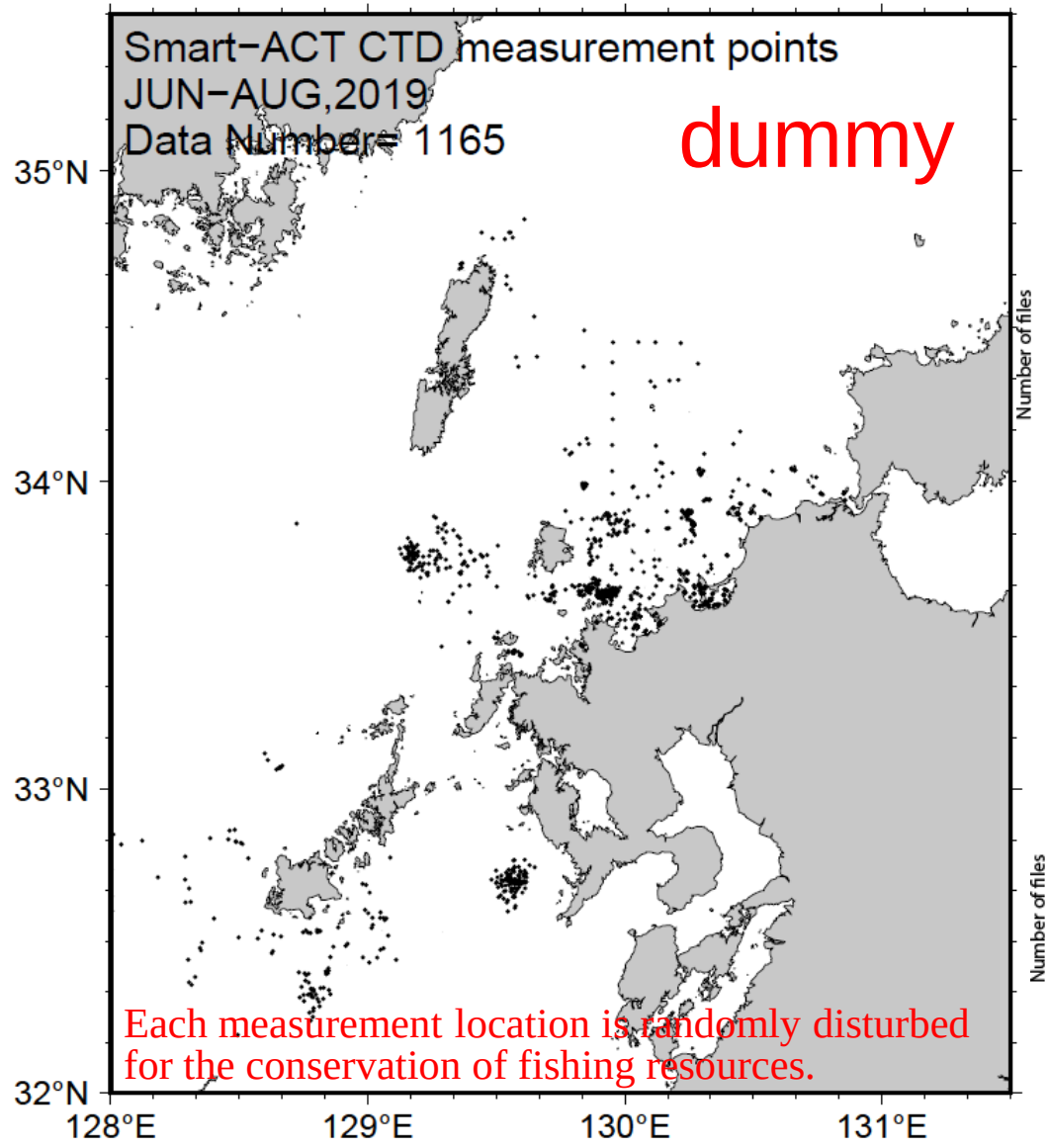

ADCP data

x4.5 from 2018 to 2021

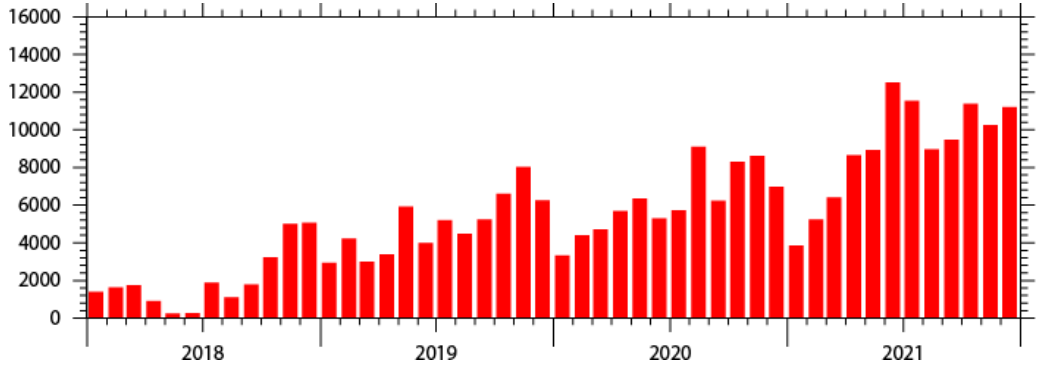

CTD data

x2.8 from 2019 to 2021

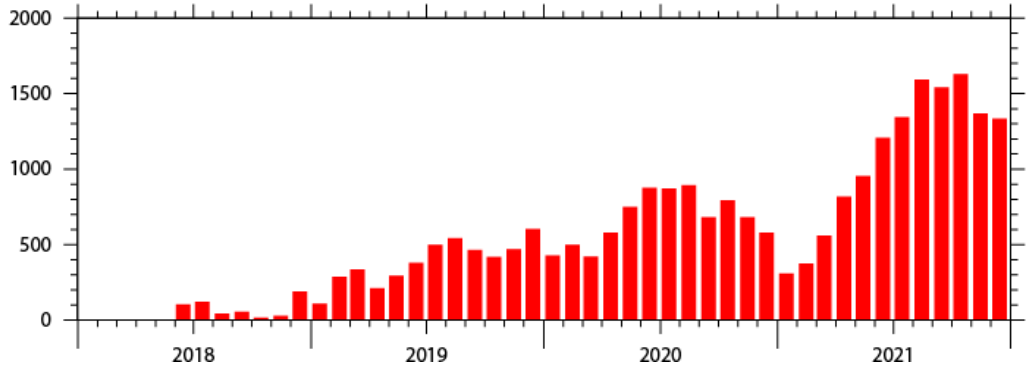

Their motivations

“Based on my CTD castings, I found the range of bottom temperature for good catches.”

“Prediction of high-frequency changes of ocean current is quite accurate on this app. I can choose the best flow condition for ideal behavior of the light-weight fishing gear.”

“Visualization of ocean environment helps to teach fishing conditions for beginners.”

“I do not have to look around the fishing grounds anymore and thus 15% cut of fuel oils. It makes me so relaxed that I can take a nap on fishing site.”

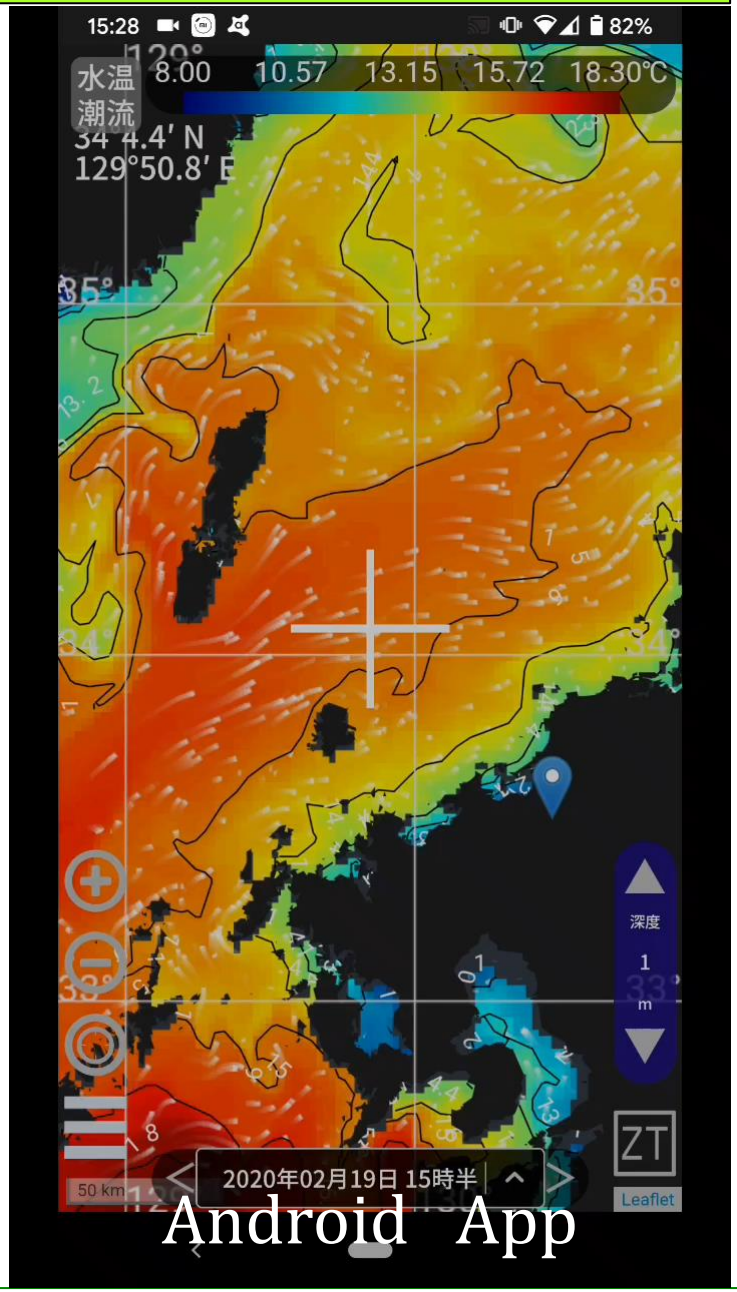

Android App

Improving tidal motion

- Observation data: F/V ADCP data
  - ✓ N=6348 from 7 vessels in Mar 2019
- Correction parameters: 4 major tide as OBC
  (Matsumoto et al., 2000, Moon et al., 2012)
  - ✓ M2: Amp×0.099, Phs–10.69°
  - ✓ S2: Amp×0.093, Phs+71.38°
  - ✓ K1: Amp×0.297, Phs+90.00°
  - ✓ O1: Amp×0.466, Phs–130.17°
- Statistics (Mar 2019)
  - ✓ r (R^2): 0.922 (0.841) → 0.944 (0.891)
  - ✓ rmsd: 8.6cm/s → 7.1cm/s

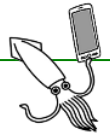

Time Series of Velocity

Along-shore component at 10m depth

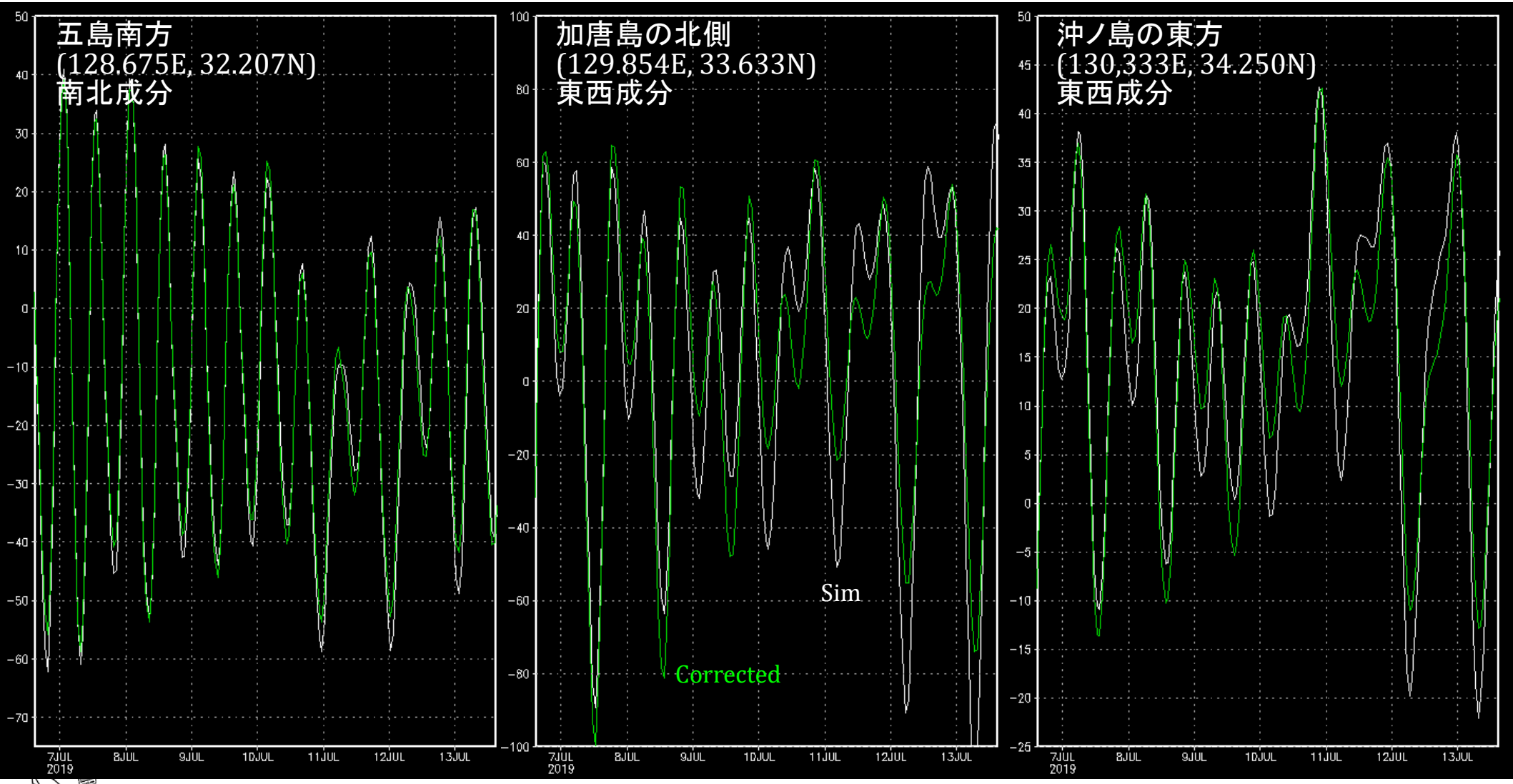

Vertical Viscosity Coefficient Increased for High-Resolution Modeling of the Tsushima/Korea Strait

NAOKI HIROSE,[a] TIANRAN LIU,[a] KATSUMI TAKAYAMA,[a] KATSUTO UEHARA,[a] TAKESHI TANEDA,[b] AND YOUNG HO KIM[c]

[a] *Research Institute for Applied Mechanics, Kyushu University, Kasuga, Fukuoka, Japan*
[b] *Fisheries Resources Institute, Japan Fisheries Research and Education Agency, Nagasaki, Japan*
[c] *Department of Oceanography, Pukyong National University, Busan, South Korea*

(Manuscript received 3 October 2020, in final form 24 April 2021)

ABSTRACT: This study clarifies the necessity of an extraordinary large coefficient of vertical viscosity for dynamical ocean modeling in a shallow and narrow strait with complex bathymetry. Sensitivity experiments and objective analyses imply that background momentum viscosity is on the order of 100 $cm^2 s^{-1}$, while tracer diffusivity estimates are on the order of 0.1 $cm^2 s^{-1}$. The physical interpretation of these estimates is also discussed in the last part of this paper. To obtain reliable solutions, this study introduces cyclic application of the dynamical response to each parameter to minimize the number of long-term sensitivity experiments. The recycling Green's function method yields weaker bottom friction and enhanced latent heat flux simultaneously with the increased viscosity in high-resolution modeling of the Tsushima/Korea Strait.

KEYWORDS: Coastal flows; Optimization; Regional models; Subgrid-scale processes

1. Introduction

Subgrid-scale parameterization is a crucial component of ocean modeling. For example, the mixing effect of mesoscale eddy motion on order of a few hundred kilometers has frequently been incorporated using the isopycnal diffusion scheme of Gent and McWilliams (1990) or subsequent versions. A similar effect may be realized through transformation of the Eulerian formulation, as derived by Zhao and Vallis (2008). The parameterization of mesoscale eddies in large-scale, non-eddy-resolving models has been a central issue in ocean general circulation modeling over the last few decades. It is also essential to parameterize vertical mixing in hydrostatic ocean models. Especially, the surface mixing has been represented well by elaborate transport schemes of turbulent kinetic energy (e.g., Large et al. 1994; Noh and Kim 1999).

At present, submesoscale or finer parameterization must be considered due to the rapid increase in model resolution, as unresolved physics will exist at any grid size. To date, the parameterization of submesoscale variability has been discussed mainly in terms of the surface mixing processes in the open ocean (e.g., Fox-Kemper et al. 2008), but the motions in coastal

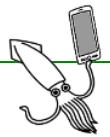

wide frequency of motions has been observed at the strait (Ostrovskii et al. 2009). The generation of internal tide (Jeon et al. 2014) leads to vertical mixing that may require some subgrid-scale parameterizations for hydrostatic ocean models.

The major objective of this study is to inversely estimate major parameters such as viscosity or diffusion coefficient aiming at appropriate values for high-resolution coastal ocean modeling. The model's sensitivity to vertical viscosity and diffusion coefficients is shown in the earlier section of this paper. However, the inverse solutions of internal parameters may interact with boundary conditions, as dynamic changes in a shallow and small domain are easily affected by surface and lateral forcings. Thus, external conditions and internal parameters must be calibrated simultaneously.

Inverse estimation of multiple parameters including the forcing conditions can be implemented through adjoint or ensemble methods, but such algorithms tend to be complex (e.g., Jordi and Wang 2013; Wang et al. 2018). A more serious problem may be their computational demand, which easily exceeds 100 times of a forward model. On the other hand, Green's functions can be readily applied to optimizing the parameters of ocean general circulation models (e.g., Menemenlis

Unfortunately, the amount of correction appeared to depend on the amount of perturbation. The expected cost function reduction also differed; the former case reduced the cost function by 23%, while the latter improved it by 33%.

The vertical diffusion coefficient (P14) increased, and the two estimates differed significantly. Notably, the present inverse estimation method was not very reliable due to its strong dependence on the level of perturbation. The 1-yr period of analysis used here may also have been too short to provide stable solutions.

b. Recycling over multiple years

1) RECYCLING METHOD

The computational demand of the long-term inverse estimation is quite high. For example, the 18 sensitivity experiments to generate the exact Green's function matrix for 10 years require $300 \times 18 = 5400$ h of calculation time. Here, we introduce the concept of recycling Green's functions (RGF) to reduce the computational burden of this process.

The right-hand side of Eq. (2) can be decomposed to measurement and dynamical portions as

$$e_j g_j = \mathcal{H}\left\{ \begin{bmatrix} \mathbf{x}_j(t_0) \\ \vdots \\ \mathbf{x}_j(t_N) \end{bmatrix} - \begin{bmatrix} \mathbf{x}_0(t_0) \\ \vdots \\ \mathbf{x}_0(t_N) \end{bmatrix} \right\}, \tag{5}$$

where $\mathcal{H}$ is the measurement operator, and $\mathbf{x}_0$ and $\mathbf{x}_j$ are the state vectors of the CTL and jth sensitivity experiments, respectively. Equation (5) can be simplified symbolically as

$$e_j g_j = \mathcal{H}\Delta\mathbf{x}_j, \tag{5′}$$

where the term $\Delta\mathbf{x}_j$ indicates the difference in the full outputs of the two experiments for a certain period.

Cyclic phenomena in the ocean such as tidal constituents, diurnal change, and seasonal variations are common in the ocean (e.g., Fukumori et al. 1998). In nature, these changes are repeated regularly, and thus the full difference $\Delta\mathbf{x}_j$ may also be repeated with each cycle. Thus, the number of model outputs in time (N) must be sufficient to resolve these cycles.

This study explores the possibility of "recycling" the use of $\Delta\mathbf{x}_j$ for seasonal cycles. In this case, the period of $\Delta\mathbf{x}_j$ should be 1 year. We used daily model outputs for fiscal year 2014 as the reference case, as it had the smallest root-mean-square dif-

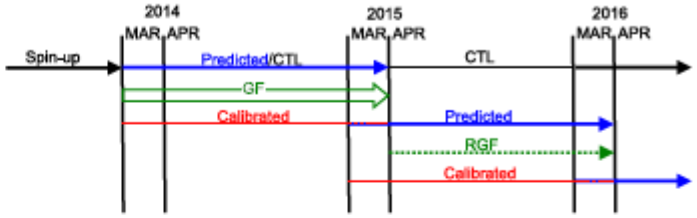

FIG. 7. Sequence of calibration for multiple parameters in the preliminary experiment (GP).

on the difference between the observation and new prediction, rather than the CTL experiment.

2) PRELIMINARY EXPERIMENT (GP)

Optimization for the first year, 2014, was already described as the first set of solutions in section 5a. After performing a new experiment for the same year using the calibrated parameters, the prediction experiment for the following year is conducted, as shown in Fig. 7. The predicted estimates become the baseline for inverse estimation in fiscal year 2015. Thus, the analysis for 2014 is optimized with exact Green's functions, but calibration for the following years is suboptimal based on the approximate Green's functions. The overlap period is one month (March) for the sequential experiments based on a rough timescale estimation of domain size (~500 km) divided by advection speed of the Tsushima Warm Current (0.2–0.5 m s^{-1}).

To maintain parameter stability, a parameter used for prediction remains unchanged if the correction was smaller than its estimated error range. When the correction for a parameter is larger than its error range, the minimum calibration is applied within the range of uncertainty. For example, the median value of the calibration factor for shortwave radiation (P7) was determined to be 0.994, as shown in Table 2. As a 0.6% reduction from the baseline condition could not be distinguished from the standard error range (±0.9%), the solar radiation was not changed for the modified experiment. For the precipitation rate (P10), a reduction of 1.0% was applied to the modified experiment as the most conservative calibration level within the range of 2.1% ± 1.1% relative to the previous configuration.

The results of vertical viscosity estimation through sequential correction are indicated by the red curve in Fig. 8. The coefficient was corrected upward, but remained at the lower limit of the estimated range. This parameter was unchanged for the fiscal year 2017, as the new estimate was statistically in-

Weaker C_S at boundary

- ✓ S Murakami, A Mochida, K Hibi, Three-dimensional numerical simulation of air flow around a cubic model by means of large eddy simulation, *J. Wind Engineering and Industrial Aerodyn.*, 25, 291-305 (1987)
- ✓ 堀内潔, LESにおけるSGS渦粘性係数のモデリング, *生産研究*, 44, 2, 93-96 (1992)
- ✓ E Balaras, C Benoeei, U Piomelli, Finite-difference computations of high Reynolds number flows using the dynamic subgrid-scale model, *Theoret. Comput. Fluid Dyn.*, 7, 207-216 (1995)
- ✓ M Chamecki, C Meneveau, M B Parlange, The local structure of atmospheric turbulence and its effect on the Smagorinsky model for Large Eddy Simulation, *J. Atmos. Sci.*, 1941-1958 (2007)

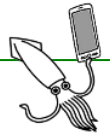

Sensitivity to BC of C_s

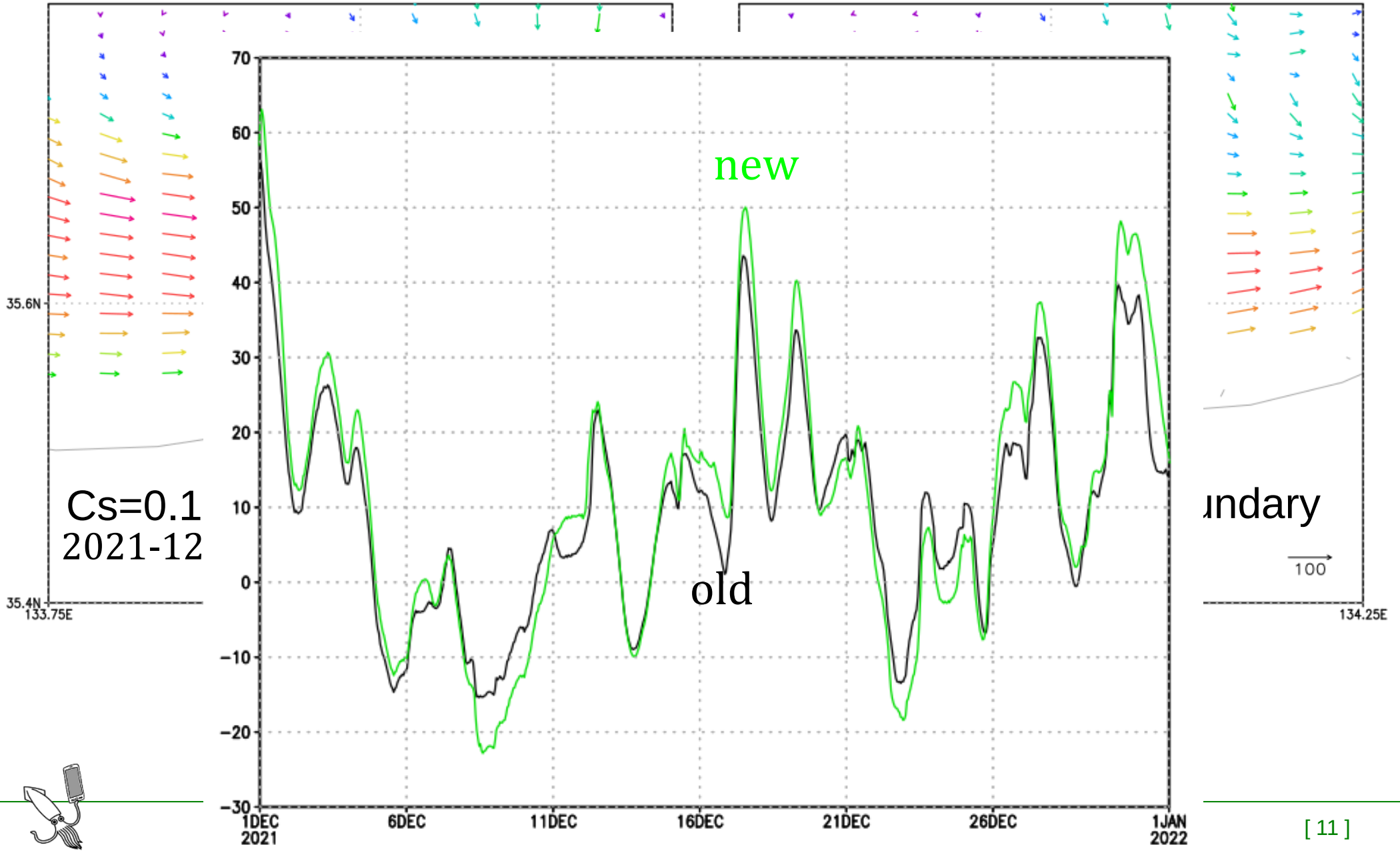

Weaker viscosity at wall boundary

Cs=0.17 everywhere

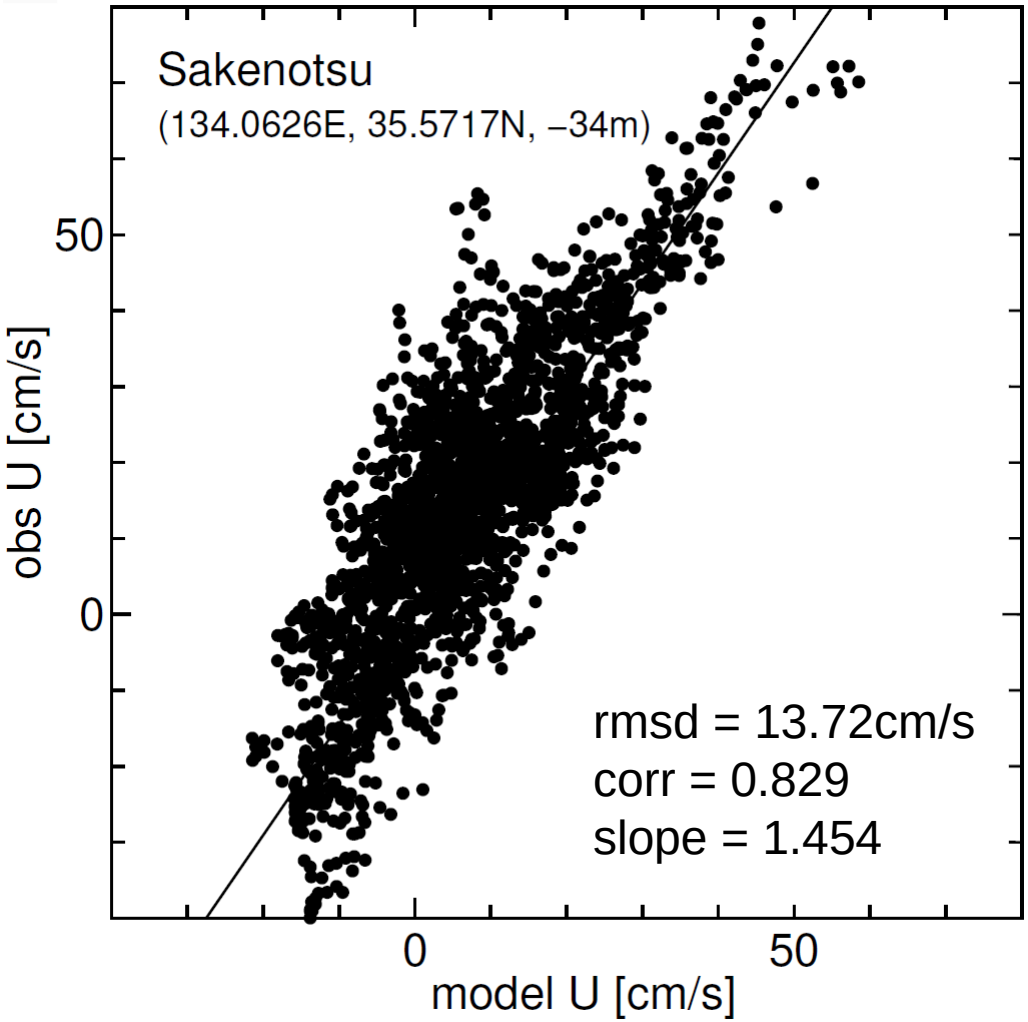

Cs=0.17 but half at boundary

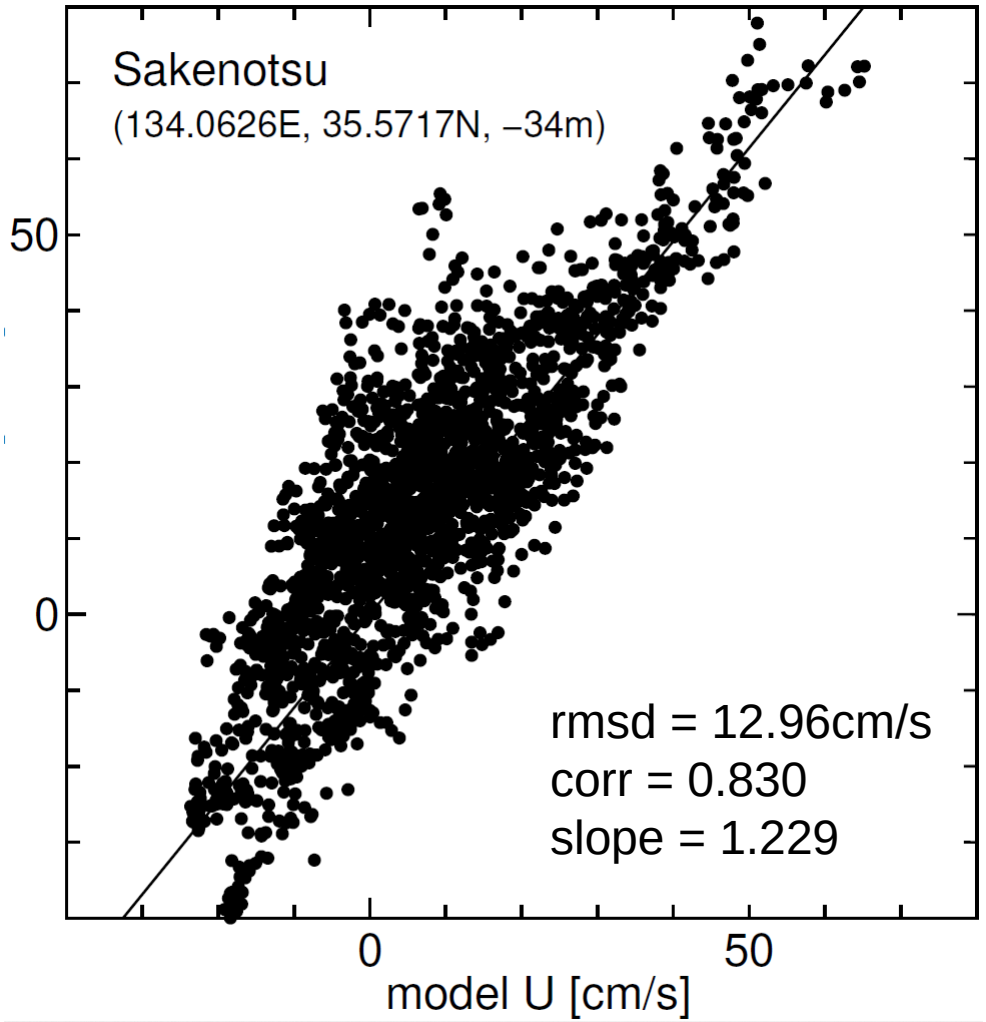

Western Channel of TKS

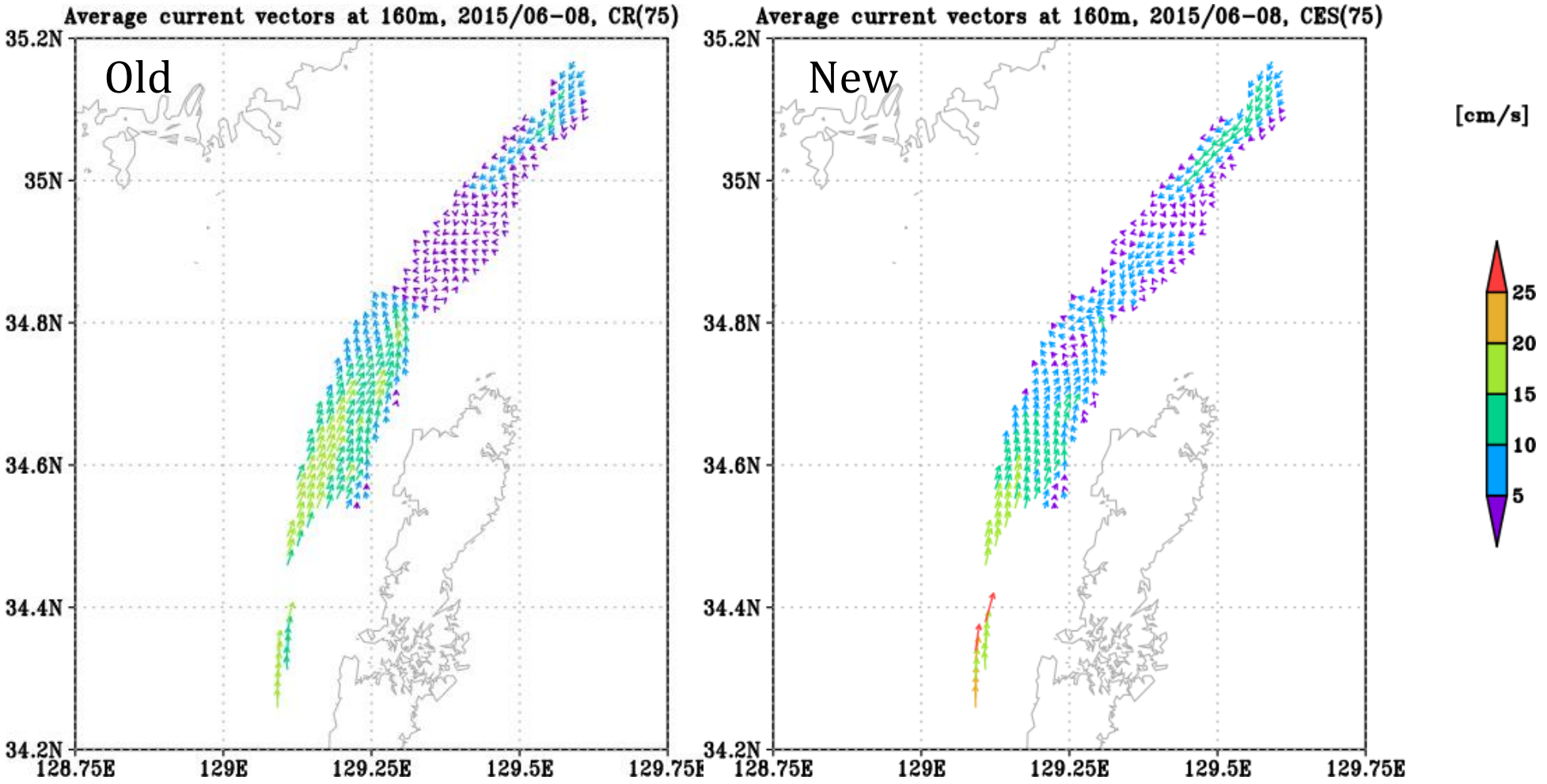

Bottom Temperature

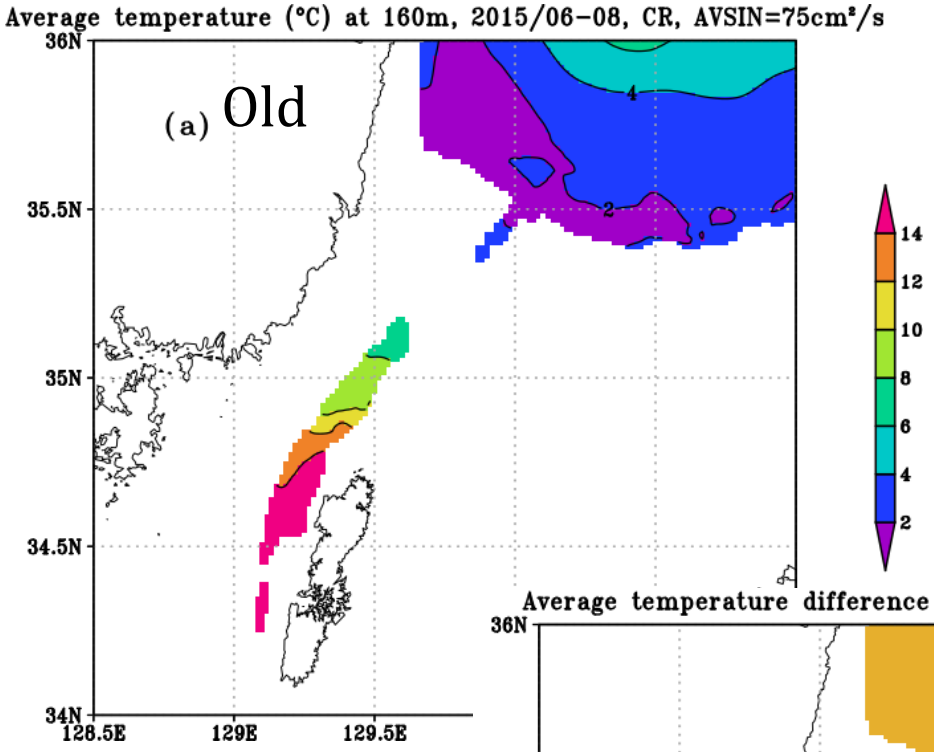

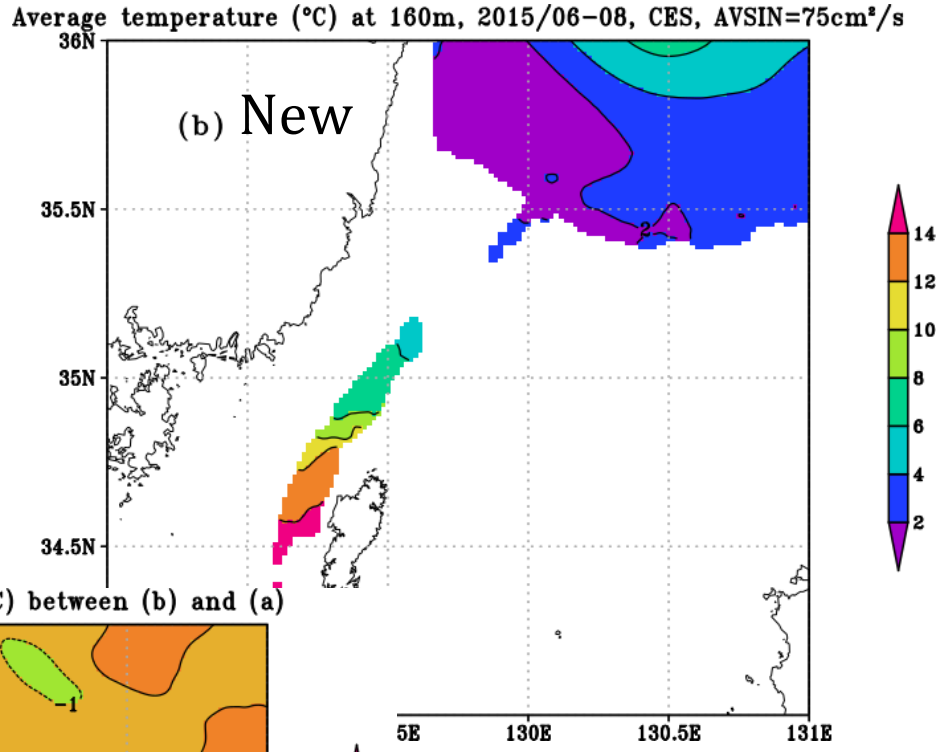

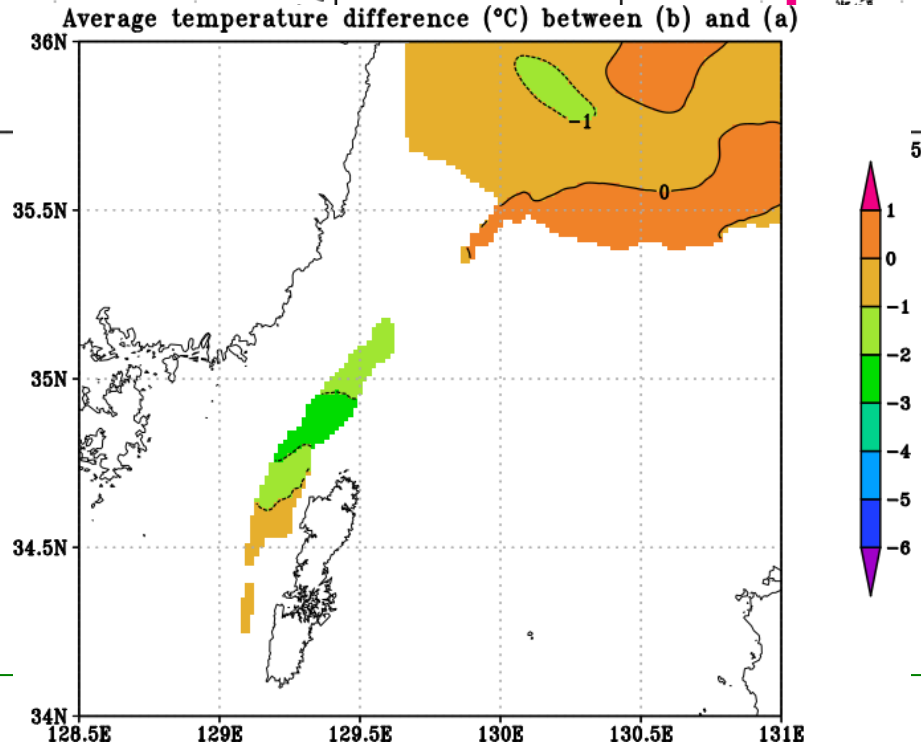

Time series of Temperature

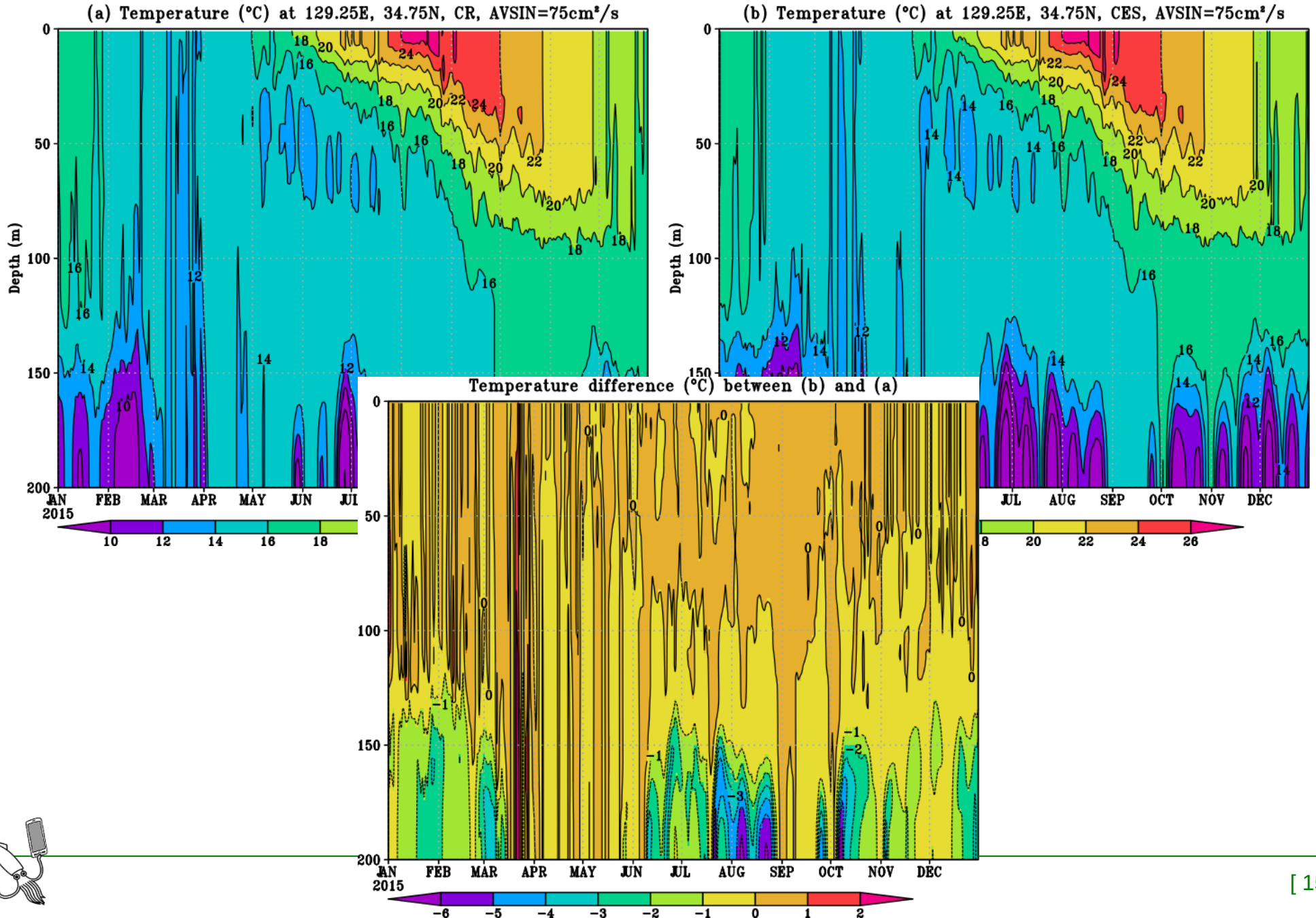

Weaker C_S at boundary

- ✓ S Murakami, A Mochida, K Hibi, Three-dimensional numerical simulation of air flow around a cubic model by means of large eddy simulation, *J. Wind Engineering and Industrial Aerodyn.*, 25, 291-305 (1987)
- ✓ 堀内潔, LESにおけるSGS渦粘性係数のモデリング, *生産研究*, 44, 2, 93-96 (1992)
- ✓ E Balaras, C Benoeei, U Piomelli, Finite-difference computations of high Reynolds number flows using the dynamic subgrid-scale model, *Theoret. Comput. Fluid Dyn.*, 7, 207-216 (1995)
- ✓ M Chamecki, C Meneveau, M B Parlange, The local structure of atmospheric turbulence and its effect on the Smagorinsky model for Large Eddy Simulation, *J. Atmos. Sci.*, 1941-1958, 2007

Applicable to coastal ocean model

Sparse KF

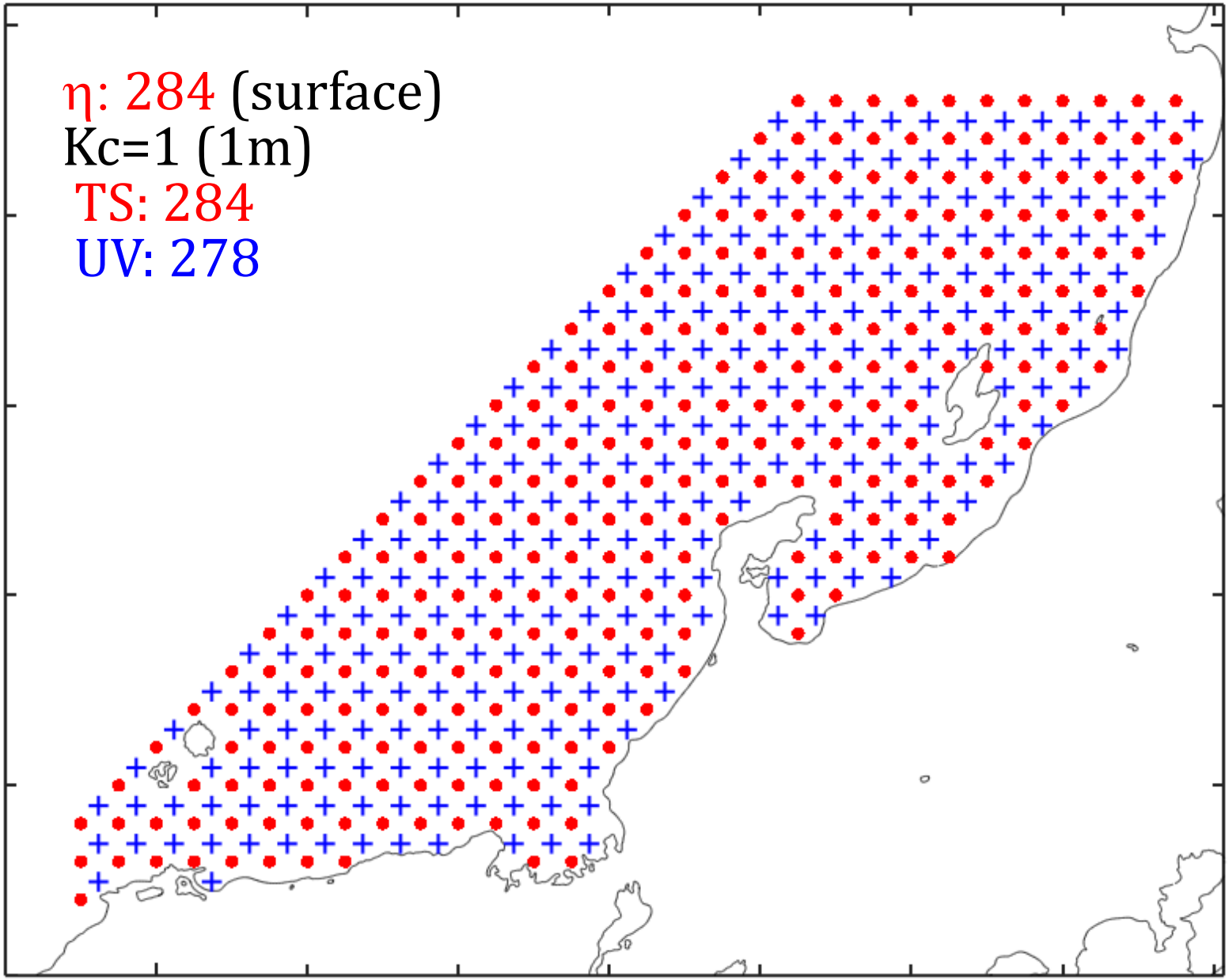

Sparse KF (unstructured)

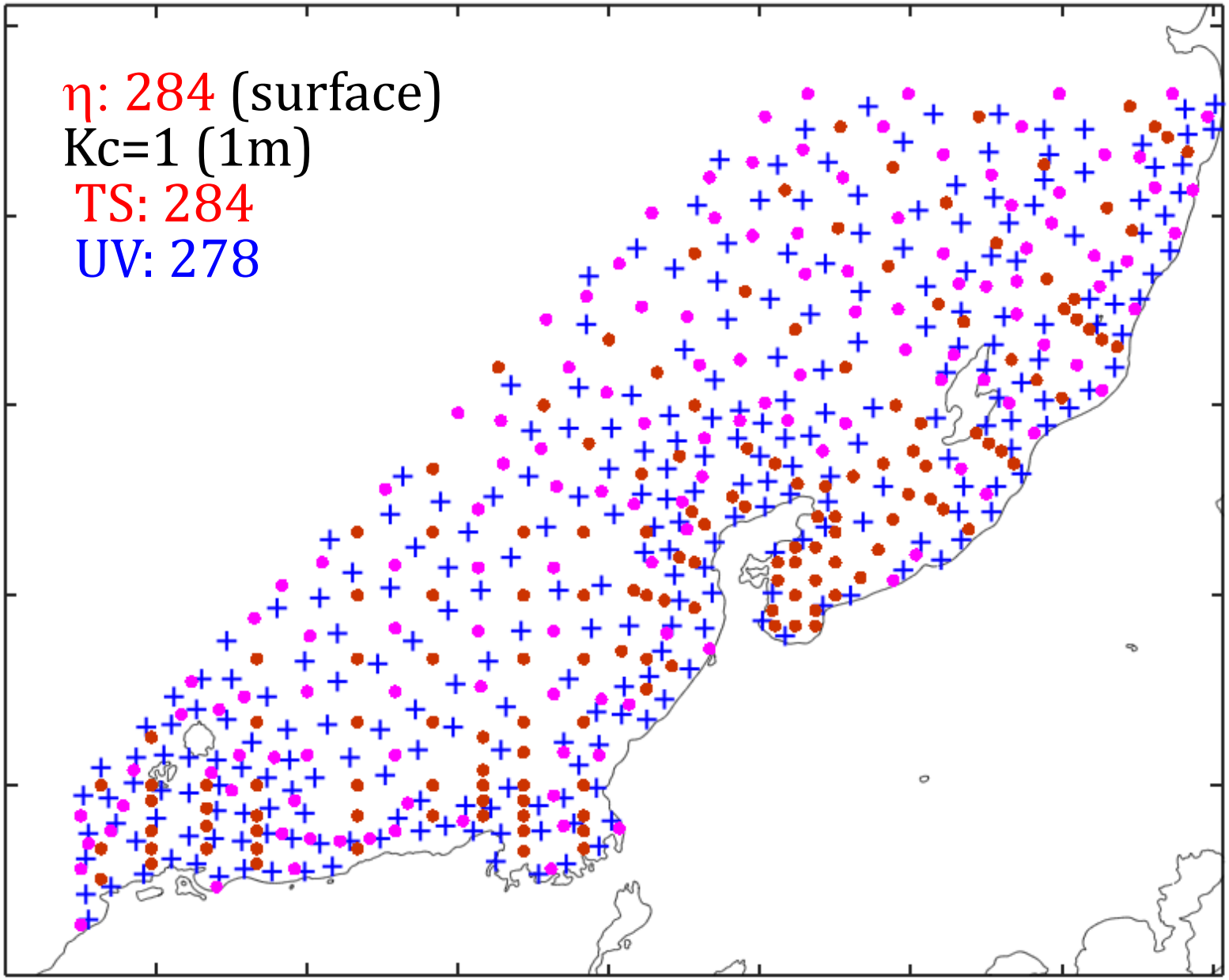

Measurement Update (Increment)

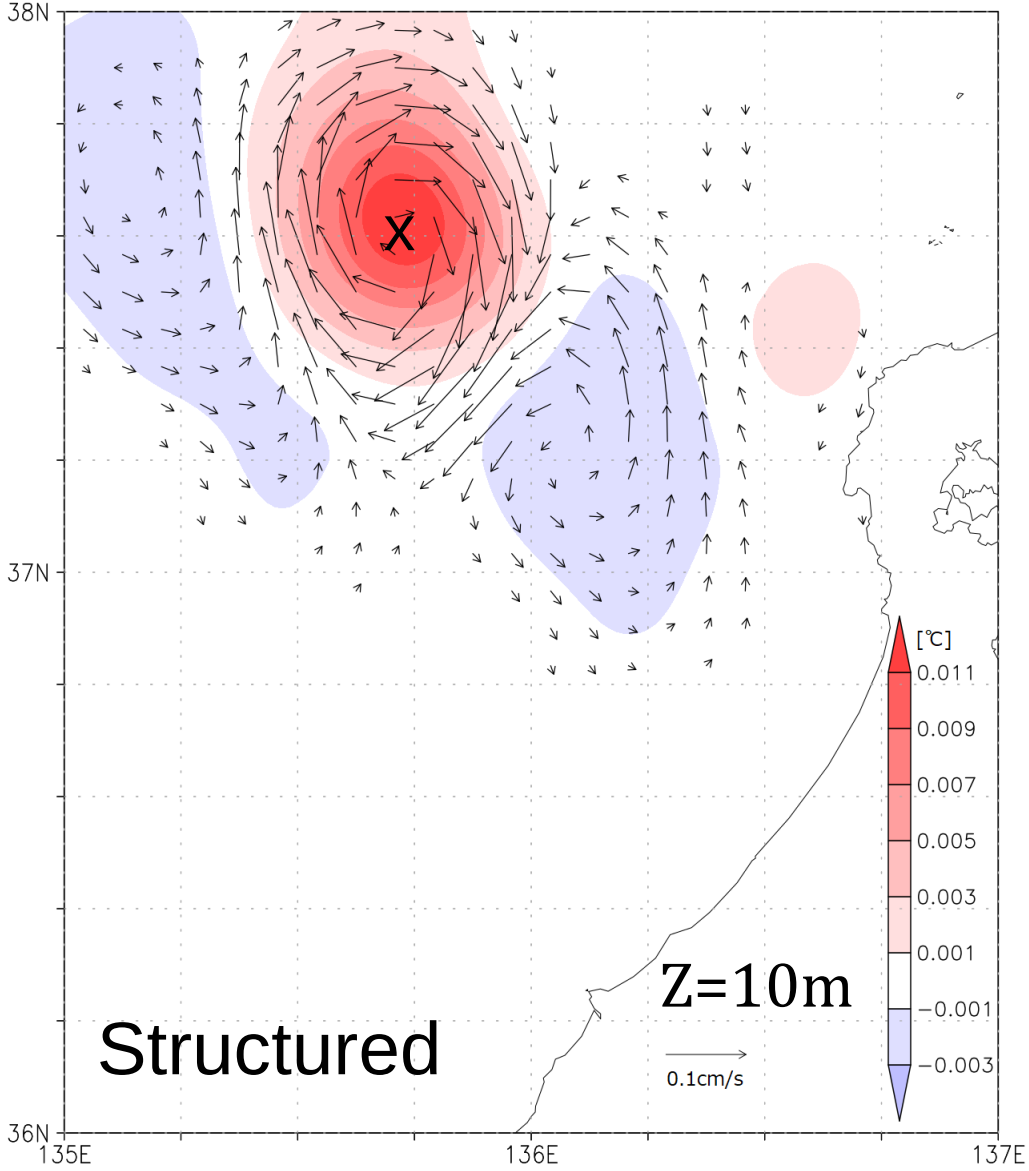

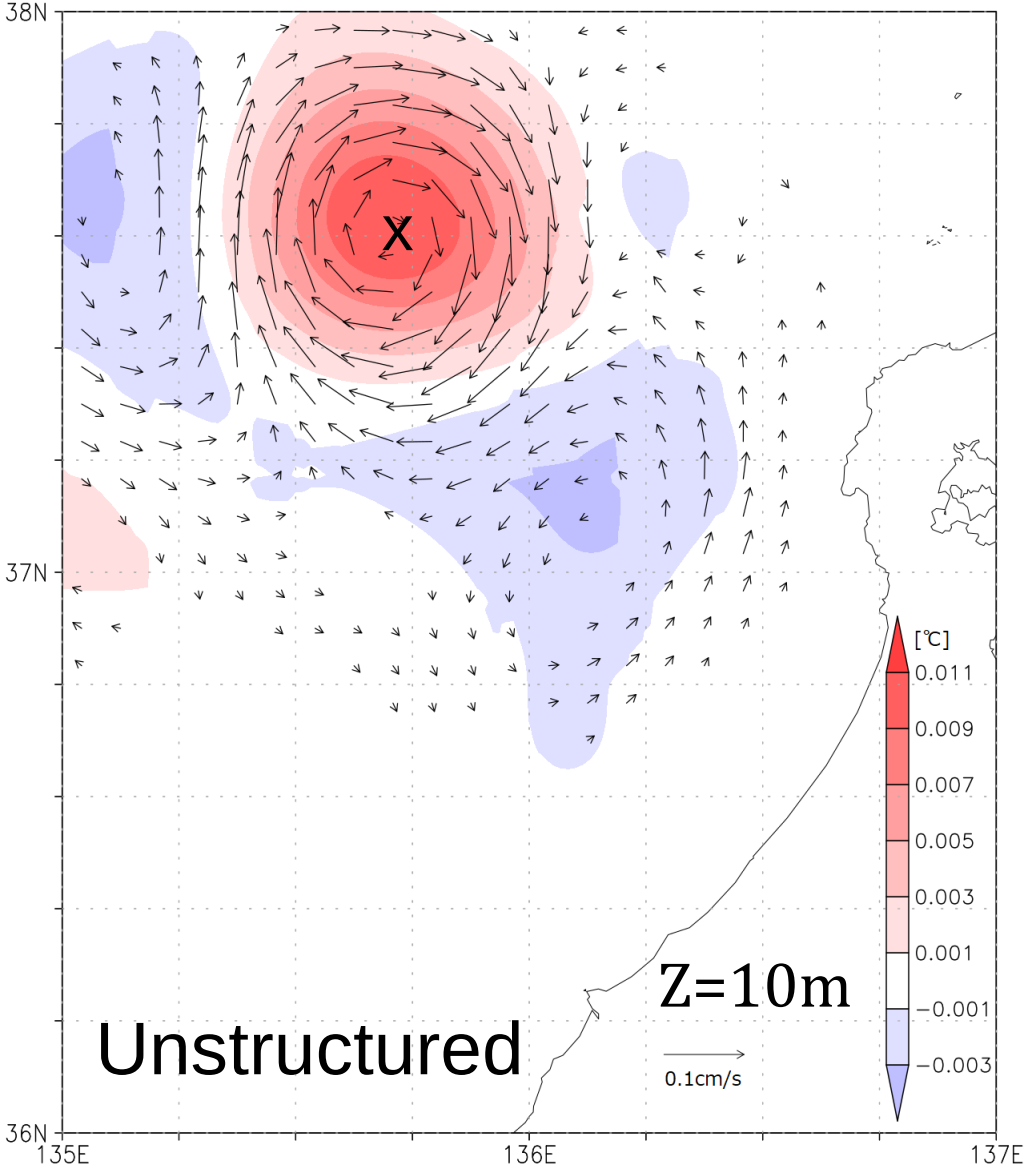

Measurement Update (Increment)

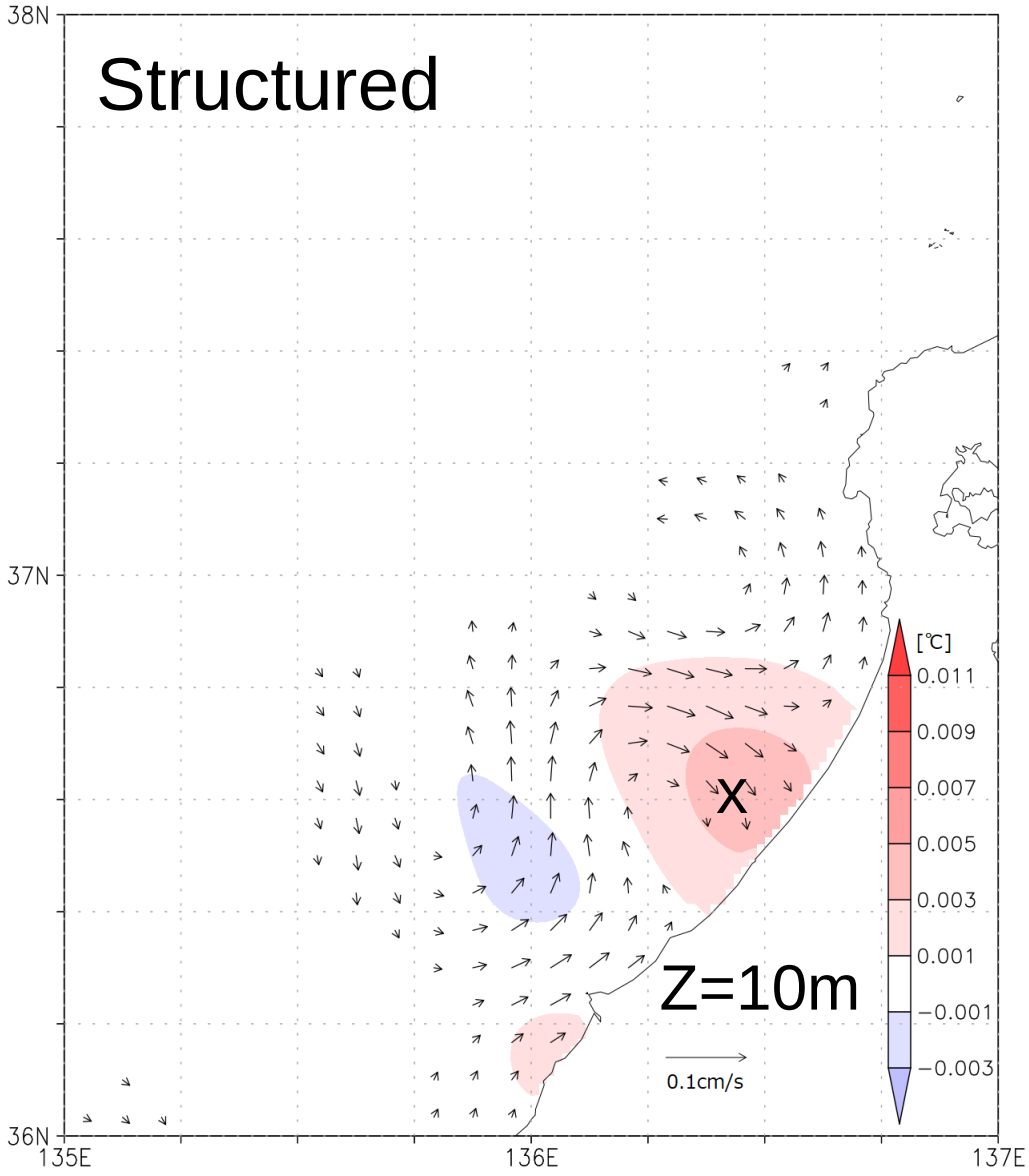

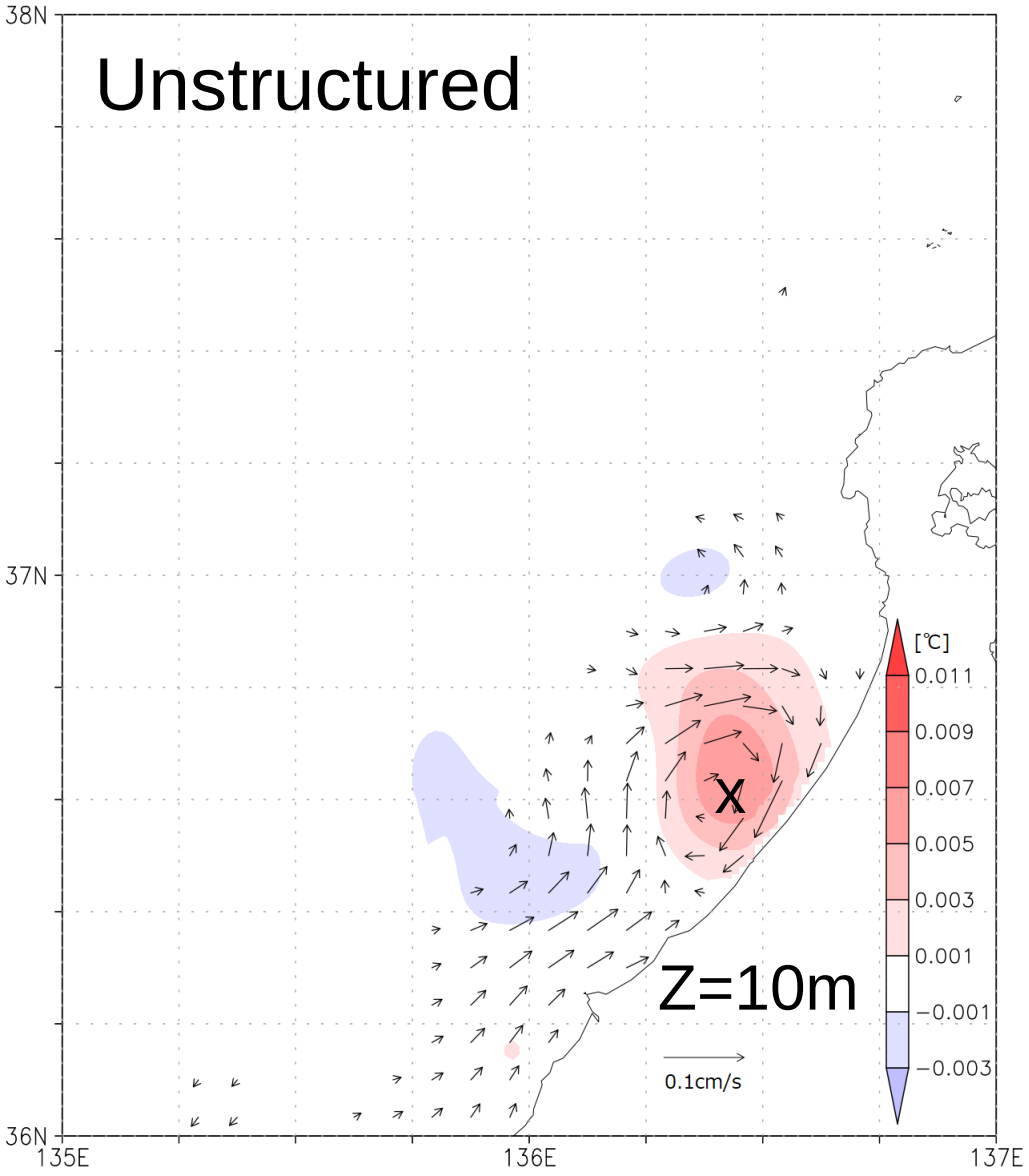

Residual variances (cm^2)

Experiment	Rvar (mup)	Rvar (dup)	Ivar
NA	40.229	40.229	0
S	31.652	36.718	1.145
U	32.374	37.461	1.145
SU	31.410	36.532	1.144
US	32.711	37.878	1.146

(2019.04-2022.03)

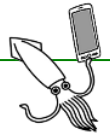

Reduction in residual variance

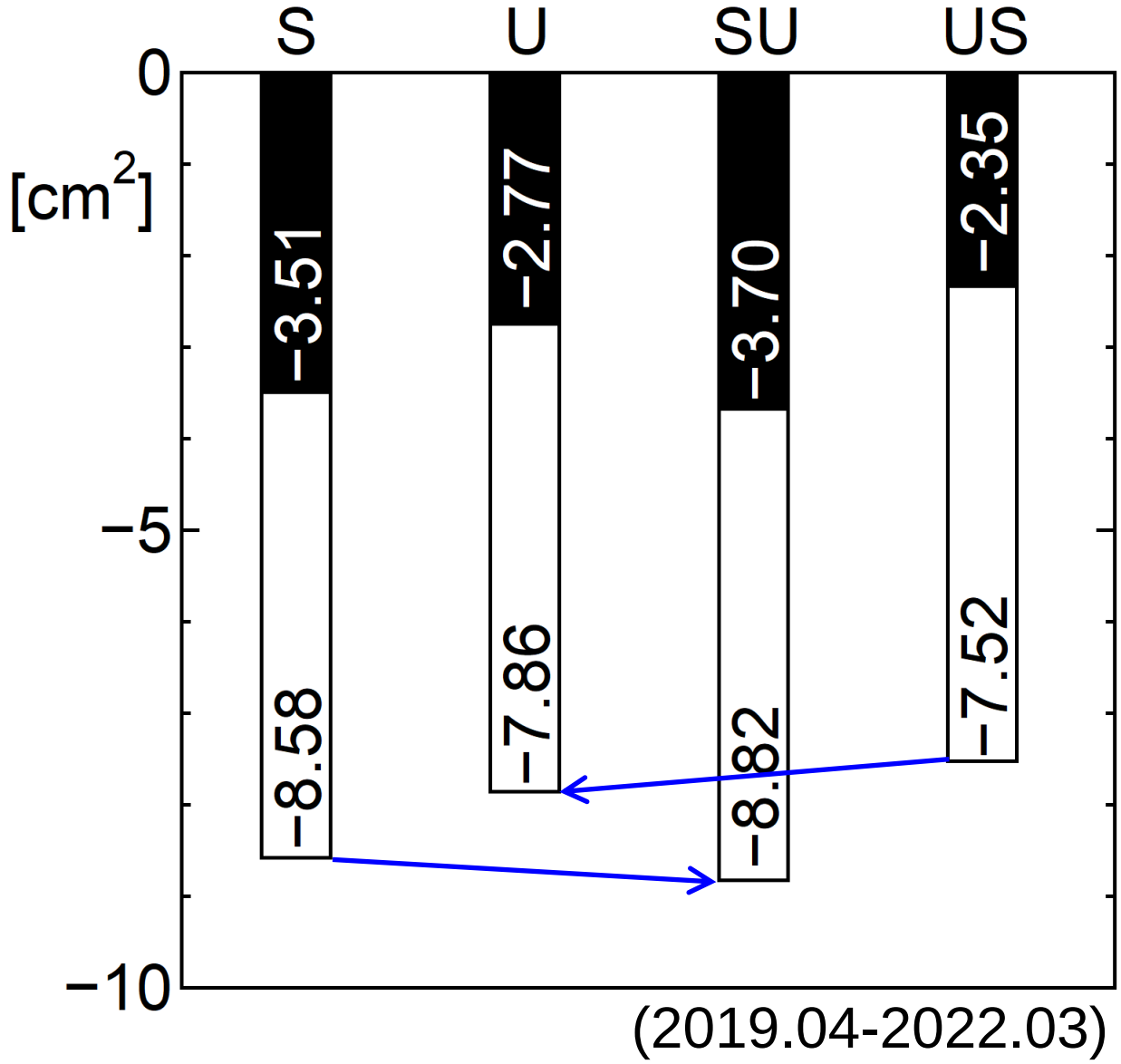

Comparison to independent data

DR_C (old)

DR_Cp (U)

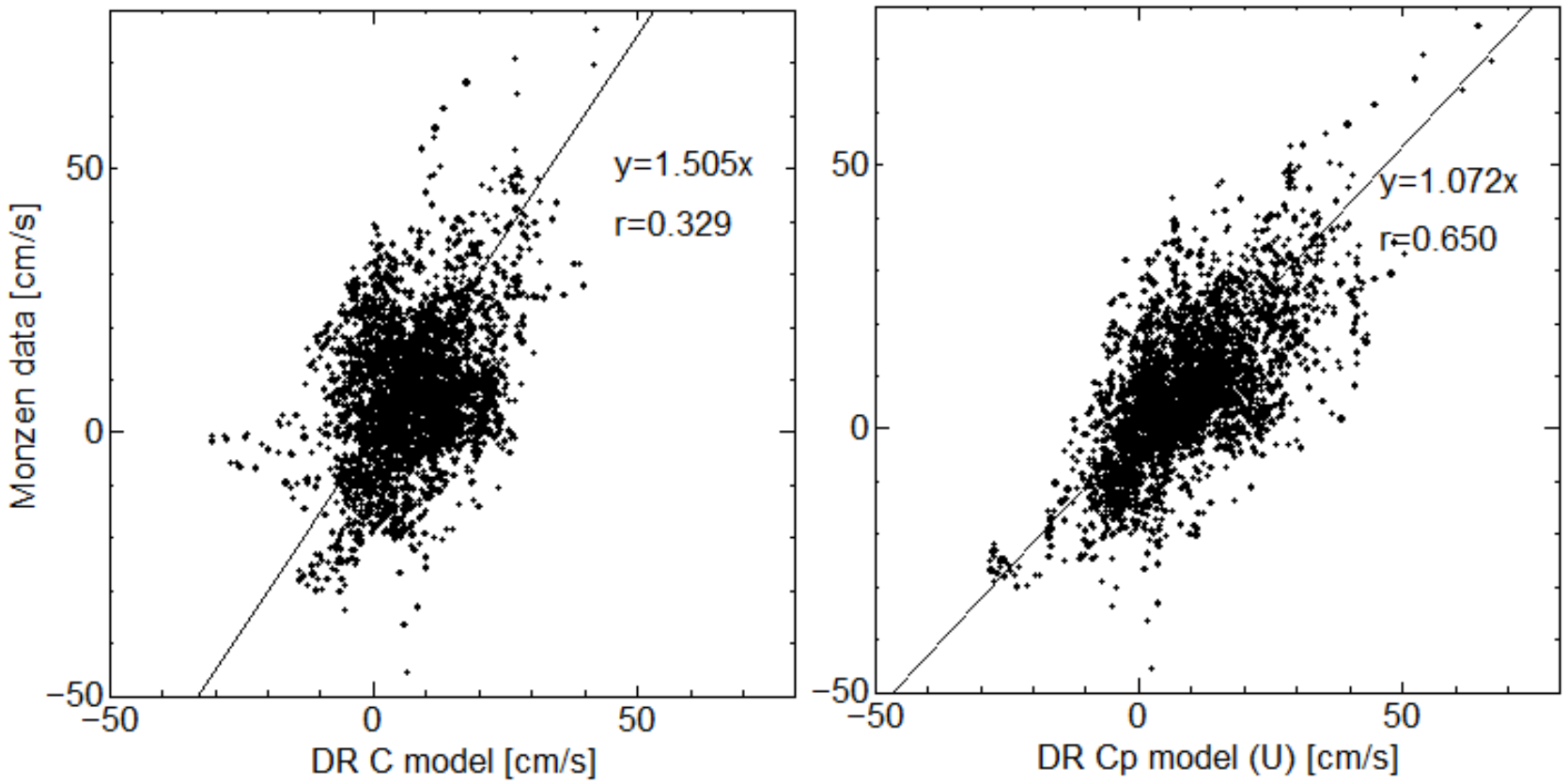

@10m, 2021.07-11

Summary

- We built win-win relationship
  - ✓ Large number of in-situ data from small fishing vessels improve coastal ocean models.
  - ✓ Fishing activity depends on the accurate prediction of coastal water motion.

- Coastal DA models updated
  - ✓ Horizontal Cs should be weaker (~60%) at land-sea boundary.
  - ✓ Sparse grid system for error covariance calculation can be unstructured for velocity components.